

ARTICLE

Open Access

Na⁺/Ca²⁺ exchanger 1 on nuclear envelope controls PTEN/Akt pathway via nucleoplasmic Ca²⁺ regulation during neuronal differentiation

Agnese Secondo¹, Alba Esposito¹, Tiziana Petrozziello¹, Francesca Boscia¹, Pasquale Molinaro¹, Valentina Tedeschi¹, Anna Pannaccione¹, Roselia Ciccone¹, Natascia Guida², Gianfranco Di Renzo¹ and Lucio Annunziato^{1,2}

Abstract

Nuclear envelope (NE) is a Ca²⁺-storing organelle controlling neuronal differentiation through nuclear Ca²⁺ concentrations ([Ca²⁺]_n). However, how [Ca²⁺]_n regulates this important function remains unknown. Here, we investigated the role of the nuclear form of the Na⁺/Ca²⁺ exchanger 1 (nuNCX1) during the different stages of neuronal differentiation and the involvement of PTEN/PI3K/Akt pathway. In neuronal cells, nuNCX1 was detected on the inner membrane of the NE where protein expression and activity of the exchanger increased during NGF-induced differentiation. nuNCX1 activation by Na⁺-free perfusion induced a time-dependent activation of nuclear-resident PI3K/Akt pathway in isolated nuclei. To discriminate the contribution of nuNCX1 from those of plasma membrane NCX, we generated a chimeric protein composed of the fluorophore EYFP, the exchanger inhibitory peptide, and the nuclear localization signal, named XIP-NLS. Fura-2 measurements on single nuclei and patch-clamp experiments in whole-cell configuration showed that XIP-NLS selectively inhibited nuNCX1. Once it reached the nuclear compartment, XIP-NLS increased the nucleoplasmic Ca²⁺ peak elicited by ATP and reduced Akt phosphorylation, GAP-43 and MAP-2 expression through nuclear-resident PTEN induction. Furthermore, in accordance with the prevention of the neuronal phenotype, XIP-NLS significantly reduced TTX-sensitive Na⁺ currents and membrane potential during neuronal differentiation. The selective inhibition of nuNCX1 by XIP-NLS increased the percentage of β III tubulin-positive immature neurons in mature cultures of MAP-2-positive cortical neurons, thus unraveling a new function for nuNCX1 in regulating neuronal differentiation through [Ca²⁺]_n-dependent PTEN/PI3K/Akt pathway.

Introduction

Nuclear Ca²⁺ concentrations ([Ca²⁺]_n) regulate many cellular functions by modulating specific proteins¹. For instance, the nuclear-targeted Ca²⁺ buffer protein parvalbumin, but not the cytosolic isoform, reduces hepatocyte proliferation². Moreover, the activation of the transcription factors Elk1³, NFAT, DREAM⁴, and CREB depends on nuclear Ca²⁺ levels. On the other hand, intranuclear Ca²⁺

dysregulation may affect cell survival, as it occurs under hypoxic conditions where it triggers the expression of proapoptotic genes^{5,6}. [Ca²⁺]_n is influenced by cytosolic Ca²⁺ levels and is regulated by the activation of specific receptors, pumps, and exchangers localized on the nuclear envelope (NE)^{7,8}. For instance, the stimulation of nuclear inositol (1,4,5)-triphosphate receptors (InsP₃R) leads to nucleoplasmic Ca²⁺ increase in isolated nuclei from *Xenopus* oocytes⁹, *Aplysia* neurons¹⁰, and pancreatic acinar cells¹¹. Furthermore, the activation of G-protein coupled receptors localized on the NE modulates—via [Ca²⁺]_n—gene

Correspondence: Lucio Annunziato (lannunzi@unina.it)

¹IRCCS SDN, School of Medicine, "Federico II" University of Naples, Naples, Italy

²IRCCS SDN, Naples, Italy

Agnese Secondo and Alba Esposito contributed equally to this work.

Edited by N. Barlev

© The Author(s) 2018



Open Access This article is licensed under a Creative Commons Attribution 4.0 International License, which permits use, sharing, adaptation, distribution and reproduction in any medium or format, as long as you give appropriate credit to the original author(s) and the source, provide a link to the Creative Commons license, and indicate if changes were made. The images or other third party material in this article are included in the article's Creative Commons license, unless indicated otherwise in a credit line to the material. If material is not included in the article's Creative Commons license and your intended use is not permitted by statutory regulation or exceeds the permitted use, you will need to obtain permission directly from the copyright holder. To view a copy of this license, visit <http://creativecommons.org/licenses/by/4.0/>.

transcription, import and export pathways of proteins, and cell cycle¹². In addition, outer and inner membranes of NE are provided with K^+ , Cl^- , and R-type Ca^{2+} channels^{13–15}, Na^+/H^+ exchanger¹⁶, Ca^{2+} -ATPase pump¹⁷, and NCX1^{18,19}. Despite the existent knowledge on the role of plasma membrane NCX in the regulation of intracellular Ca^{2+} concentrations and Ca^{2+} -dependent pathways^{20–22}, nuNCX1 function remains unexplored. Interestingly, global silencing of NCX1 prevents neurite outgrowth through the inhibition of Akt pathway thus reducing NeuN-positive neurons²³. On the other hand, it has been reported that miR-29a targeting the phosphatase and tensin homologs on chromosome ten (PTEN), increase phosphorylation of Akt, thus promoting neurite outgrowth²⁴. Indeed, deregulation of PTEN affects neurogenesis, neurite outgrowth, synaptogenesis, and synaptic plasticity^{25,26}. Therefore, the purpose of the present study has been to investigate the contribution of nuNCX1 in the modulation of nuclear-resident PTEN/PI3K/Akt pathway via $[Ca^{2+}]_n$ during neuronal differentiation.

Results

Characterization of nuNCX1 expression in neuronal cells

Immunolocalization of the NCX1 isoform in NGF-differentiated PC12 cells revealed diffused DAB immunostaining of this isoform. Together with its plasmamembrane expression, NCX1 was also present at the nuclear level (Fig. 1Aa, b, c). Furthermore, in specific NE areas, NCX1 colocalized with Lamin B1/B2 (Fig. 1Ba), a component of nuclear lamina connected with the nucleoplasmic face of the inner membrane (INM). However, when NGF-differentiated PC12 cells were transfected with siRNA against NCX1 (siNCX1), Lamin B1/B2-NCX1 co-localization disappeared (Fig. 1Ba, c). Moreover, in whole neuronal cells, NCX1 immunosignal was also found outside the nucleus (Fig. 1Ba) and disappeared in cells treated with siNCX1 (Fig. 1Bb). Confocal analysis showed a significant immunosignal of NCX1 on the NE of isolated nuclei derived from differentiated PC12 cells (Fig. 1Ca, b). Nissl staining showed the lack of ER contamination and the integrity of isolated nuclei while ethidium bromide staining confirmed the high purity of these preparations and the lack of dispersed DNA (data not shown). In addition, any possible contamination by specific markers of the plasmamembrane, mitochondria, Golgi complex, and ER such as the plasma membrane calcium ATPase, Na^+ channels, dynamin-related protein 1, GM130, and stromal interaction molecule 1 were detected in the preparation of isolated nuclei, except for the two nuclear markers H3 and Akt (data not shown).

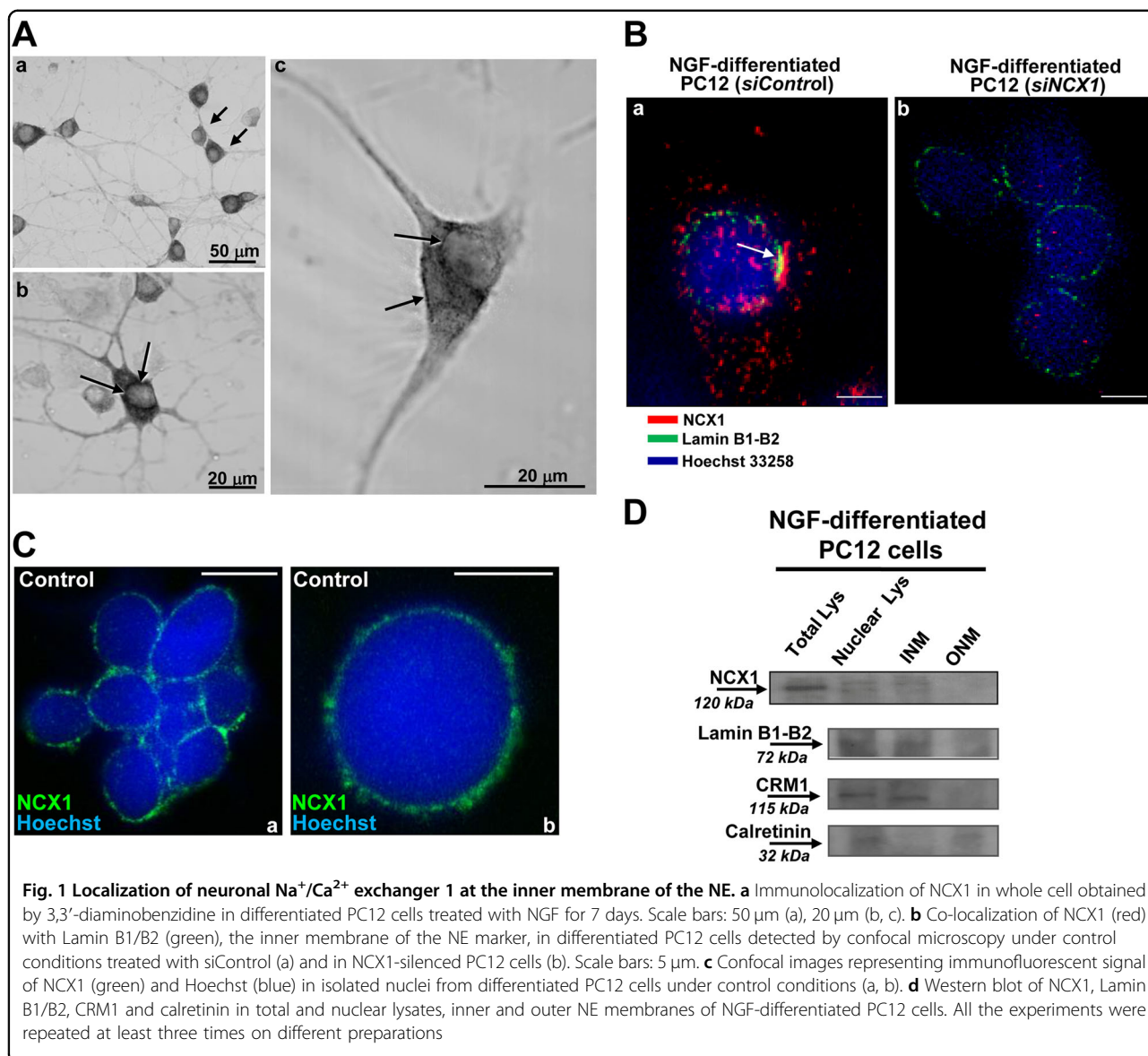
To further confirm the specific localization of NCX1 at INM level, we performed a separation between outer and inner membranes of NE with cold Na-citrate in isolated nuclei obtained from NGF-differentiated PC12 cells. Once the outer membrane was removed, NCX1 was detected by

Western blot only on the inner membrane attached to the nuclei and in total lysate of both whole cells and total nuclei (Fig. 1D). Efficient isolation of INM was confirmed by the expression of Lamin B1/B2 and CRM1, a member of nuclear transport factor family (Fig. 1D). Furthermore, only the preparation of outer NE membrane expressed calreticulin, an ER/SR protein that is contiguous with the outer NE (Fig. 1D).

Expression and function of NCX isoforms in NE

In an attempt to study the involvement of nuNCX1 in the different stages of neuronal differentiation, immunolocalization of this isoform was performed also in PC12 cells exposed to NGF for 3 days before complete differentiation. At 3 days, DAB immunostaining of NCX1 was almost totally detected in nuclear compartment (Fig. 2A, black arrow) and slightly localized in some part of plasma membrane (Fig. 2A, gray arrow). qRT-PCR experiments showed that, during differentiation with NGF, NCX1 transcripts increased in PC12 cells with a significant peak at 3 days of exposure (Fig. 2B). On the other hand, the transcripts of the third isoform of the exchanger, NCX3, significantly reduced at 3 and 7 days of exposure (in A.U. \pm SEM: control = 1.02 ± 0.03 ; 3 days NGF = 0.52 ± 0.05 * $p < 0.05$ vs. control; 7 days NGF = 0.55 ± 0.08 , * $p < 0.05$ vs. control). Moreover, Western blot analysis revealed that nuNCX1 expression in PC12 cells peaked after 3 days exposure to NGF in nuclear preparations (Fig. 2C), thus suggesting a specific role played by nuclear NCX1 in triggering differentiation at that time. By contrast, NCX3 protein expression dropped dramatically in the same preparation (data not shown).

Then, NCX1 activity was studied by exposing to a Na^+ -free solution single nuclei loaded with Fura-2AM, a fluorescent dye exclusively concentrated in NE lumen²⁷. Na^+ -free perfusion forced the exchanger to operate in the forward mode, moving Ca^{2+} from the nucleoplasm to the NE lumen. This elicited an increase of Ca^{2+} level in the NE lumen. In particular, this $[Ca^{2+}]$ increase induced by Na^+ -free exposure was much higher in nuclei obtained from PC12 cells exposed to NGF for 3 days than those exposed for 7 days or undifferentiated controls (Fig. 2D). In the same nuclear preparation, a pharmacological characterization of NCX1 activity in the forward mode was performed by the Na^+ ionophore monensin, or blocking NCX by the amiloride analog 3-amino-6-chloro-5-[(4-chloro-benzyl)amino]-n-[[[2,4-dimethylbenzyl]-amino]iminomethyl]-pyrazinecarboxamide (CB-DMB)²⁸. Whereas monensin was able to enhance the Na^+ -dependent activity of the exchanger, possibly by increasing intra-nuclear Na^+ levels, CB-DMB prevented the increase in NE Ca^{2+} level associated with NCX activation (Fig. 2E). Furthermore, NE Ca^{2+} increase was completely prevented in isolated nuclei from PC12 cells previously treated with siNCX1 (Fig. 2E).



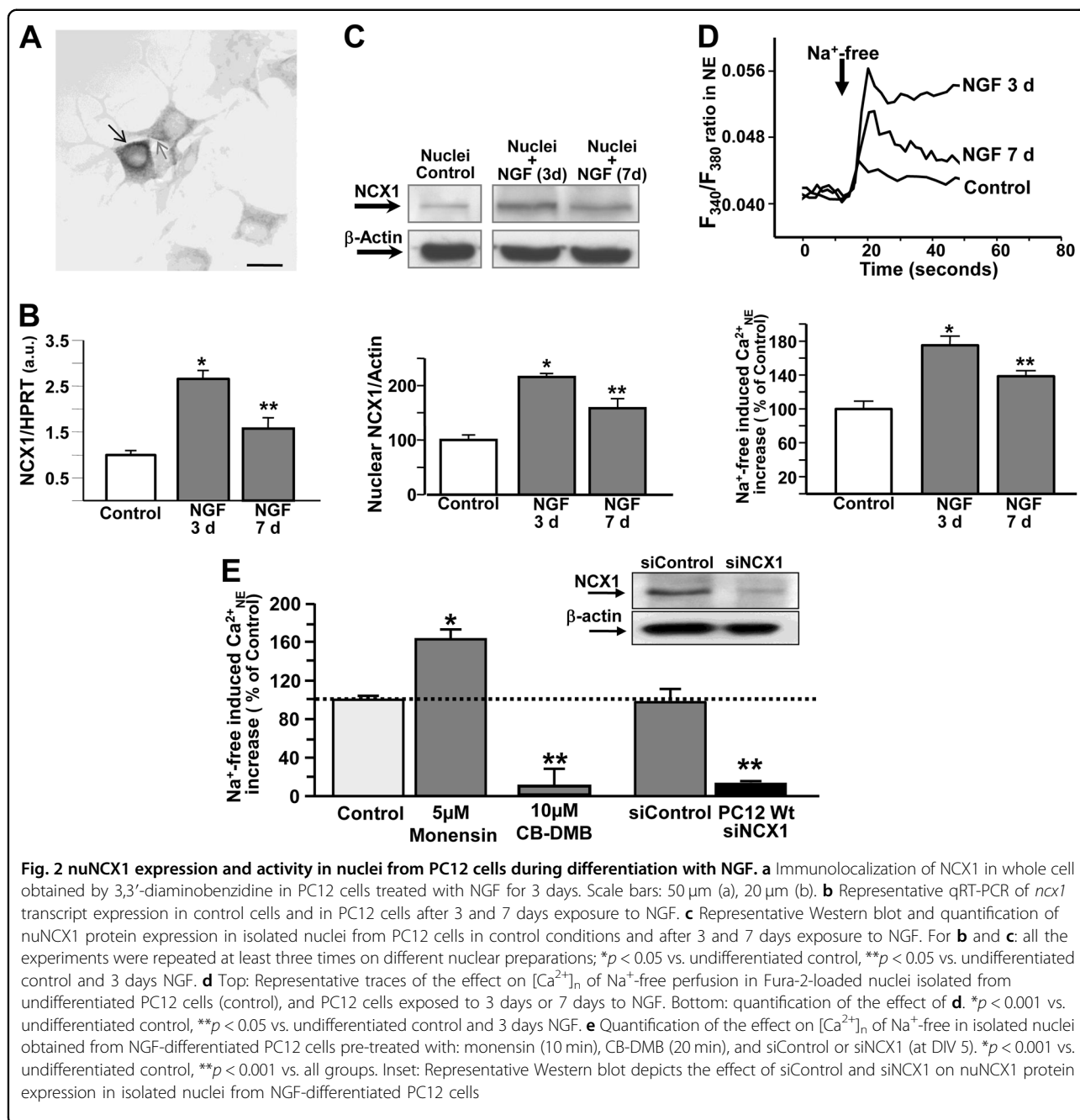
nuNCX1 silencing prevents nuclear-resident Akt phosphorylation induced by Na⁺-free perfusion

To verify whether nuNCX1 activation could modulate the phosphorylation of nuclear-resident Akt, a Ca²⁺-dependent kinase mainly involved in neurite outgrowth, we exposed isolated nuclei to a Na⁺-free solution under controlled conditions of temperature. Isolated nuclei were obtained from PC12 cells treated with NGF for 3 days, a time of the highest expression of nuNCX1 (see Fig. 2). Na⁺-free induced phosphorylation of nuclear-resident Akt in isolated nuclei from PC12 cells (Fig. 3a). Moreover, Na⁺-free-induced Akt phosphorylation was evident already after 5 min of exposure (Fig. 3a). The same activation of Akt was induced by exposing intact nuclei to bradykinin (BK) (Fig. 3a), whose Gq-coupled receptors are located on the NE inner membrane²⁹. This

effect was prevented by pre-treating nuclei for 10 min with the PI3'-K inhibitor LY294002 (25 μM) before Na⁺-free exposure (Fig. 3b). Interestingly, in nuclear preparations obtained from neuronal cells previously exposed to siNCX1, Na⁺-free perfusion (5 min) failed to induce Akt phosphorylation compared to siControl cells (Fig. 3c).

Selective inhibition of nuNCX1 by the chimeric protein XIP-NLS increases nucleoplasmic Ca²⁺ level thus limiting neuronal differentiation

Forty-eight hours after the transfection of XIP-NLS (Fig. 4a), confocal microscopy and immunoblot analysis revealed that XIP-NLS was selectively localized in the nuclei of NGF-differentiated PC12 cells (Figs. 4b, c). Indeed, EYFP signal co-localized with nuclear DNA

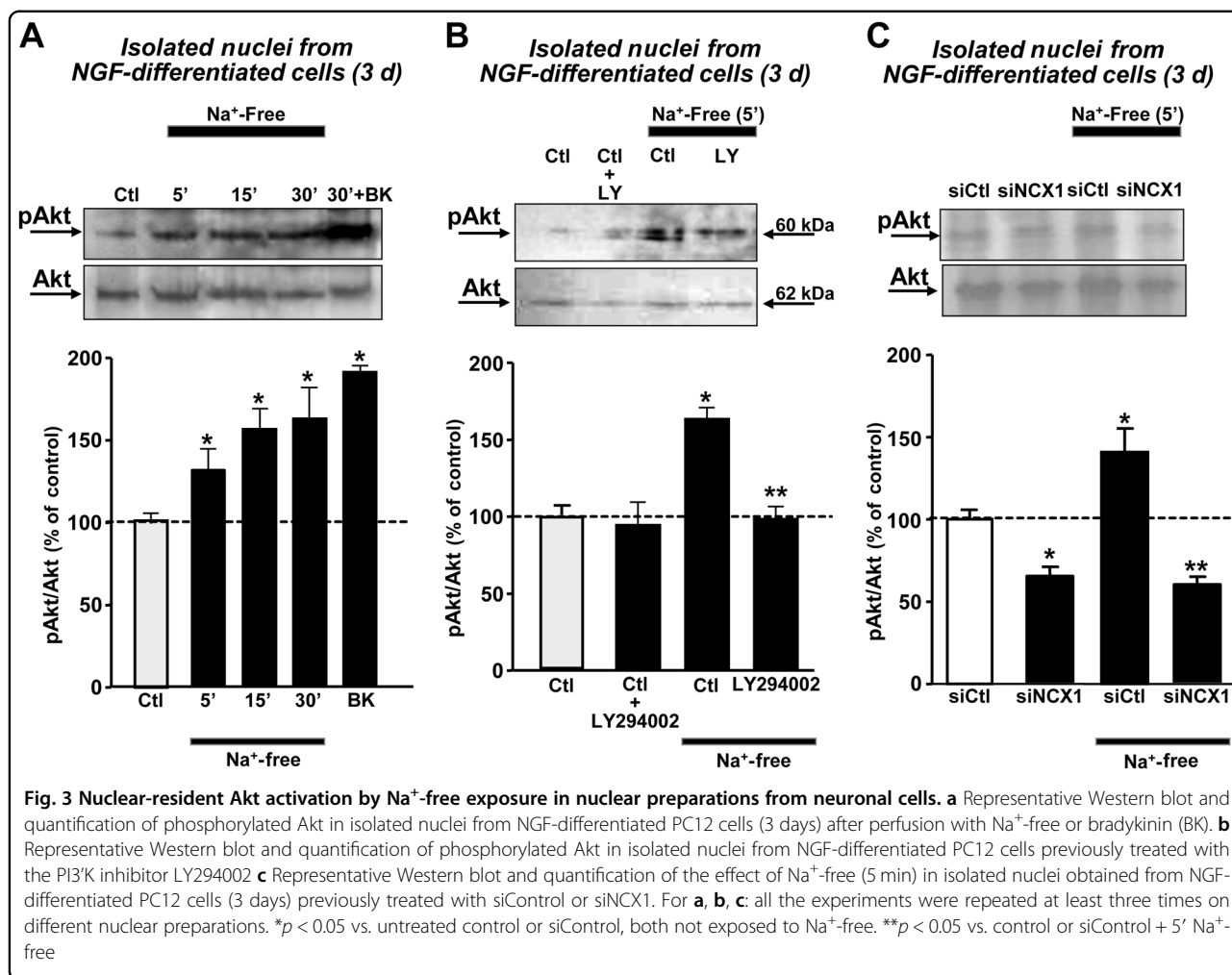


staining Hoechst 33258 in nuclei efficiently transfected with XIP-NLS (Fig. 4b). Furthermore, the specificity of the nuclear localization of XIP-NLS was revealed by the co-detection, after 48 h, with the nuclear markers CREB and pCREB in the same fraction. Further evidence for the nuclear localization of XIP-NLS and for the purity of our cellular fractions was the absence of the cytosolic protein SOD1 in the nuclear fraction (Fig. 4c).

Furthermore, XIP-NLS inhibited Na⁺-dependent nuNCX1 activity elicited by Na⁺-free perfusion in isolated nuclei obtained from NGF-differentiated PC12 cells, as

detected by Fura-2 microfluorimetry (Figs. 5a, b). By contrast, as expected by the nuclear selectivity of the chimeric protein, XIP-NLS did not affect NCX currents measured by patch-clamp at plasma membrane level in NGF-differentiated PC12 cells (Figs. 5c, d).

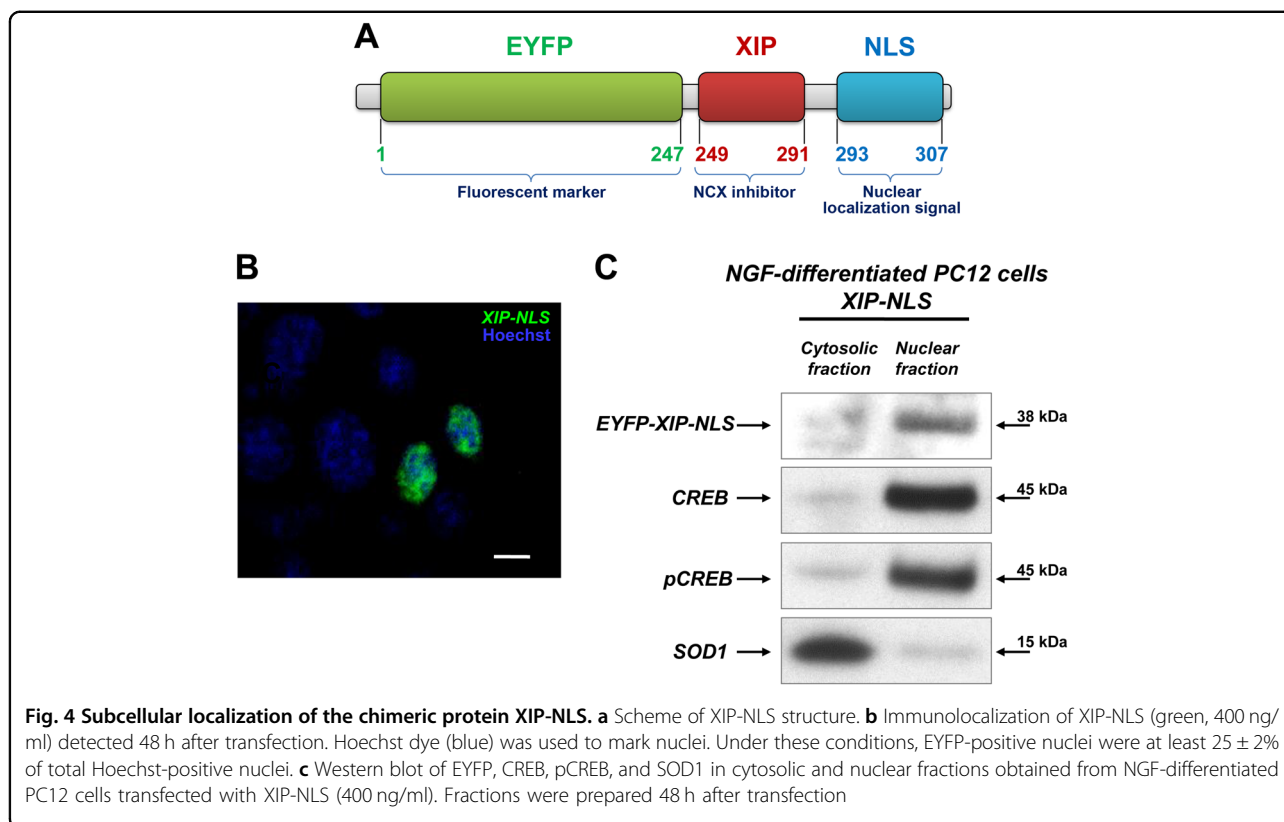
In NGF-treated PC12 cells transfected with XIP-NLS, this peptide significantly increased Fura-dextran-detected nucleoplasmic Ca²⁺ peak in response to the Gq-protein coupled receptor agonist ATP (100 μM) compared to mock control (Fig. 6a). Once transfected, XIP-NLS significantly reduced GAP-43 expression and Akt



phosphorylation in PC12 cells exposed to NGF for 3 days compared to mock control (Fig. 6b). Interestingly, under the same conditions, XIP-NLS significantly increase the expression of the negative regulator of PI3K/Akt pathway, phosphatase and tensin homolog (PTEN) (Fig. 6b), mainly involved in axonal growth modulation²⁴. Then, in accordance with the prevention of the neuronal phenotype, XIP-NLS significantly reduced TTX-sensitive Na⁺ currents in PC12 cells exposed to NGF for 3 days (Figs. 6, d). Furthermore, XIP-NLS significantly decreased membrane potential in PC12 cells exposed to NGF for 3 days compared to the respective controls (Fig. 6e).

A separation between outer and inner NE membranes of isolated nuclei obtained from primary cortical neurons showed a specific localization of NCX1 on the inner membrane attached to the nuclei (Fig. 7a). Furthermore, efficient isolation of INM in cortical neurons was confirmed by the expression of Lamin B1/B2 (Fig. 7a). On the other hand, the preparation of outer NE membrane

expressed karyopherin β2 (Fig. 7a). Interestingly, once transfected at higher concentrations in cortical neurons, XIP-NLS carrying EYFP co-immunoprecipitated with nuNCX1 as detected with anti-NCX1 in isolated nuclei (Fig. 7b). As occurred in NGF-treated PC12 cells, XIP-NLS significantly increased Fura-dextran-detected nucleoplasmic Ca²⁺ peak in response to ATP (100 μM) in cortical neurons (Fig. 7c). This suggests that XIP-NLS was able to reduce Ca²⁺ buffering properties of neuronal nuclei. Moreover, also in mature neurons (7 DIV), the chimeric protein reduced terminal differentiation markers, such as GAP-43 and MAP-2 (Figs. 7d, e), significantly increased PTEN expression and decreased Akt phosphorylation not only in total lysates (Fig. 7d, e) but also in isolated nuclei (Fig. 8a) from cortical neurons. In order to strength the evidence demonstrating the role of nuclear NCX1 isoform in the differentiation of primary cortical neurons, we analyzed the effect of the nuclear inhibitor of NCX1, XIP-NLS, on the markers of both immature and mature rat cortical neurons. To this aim we

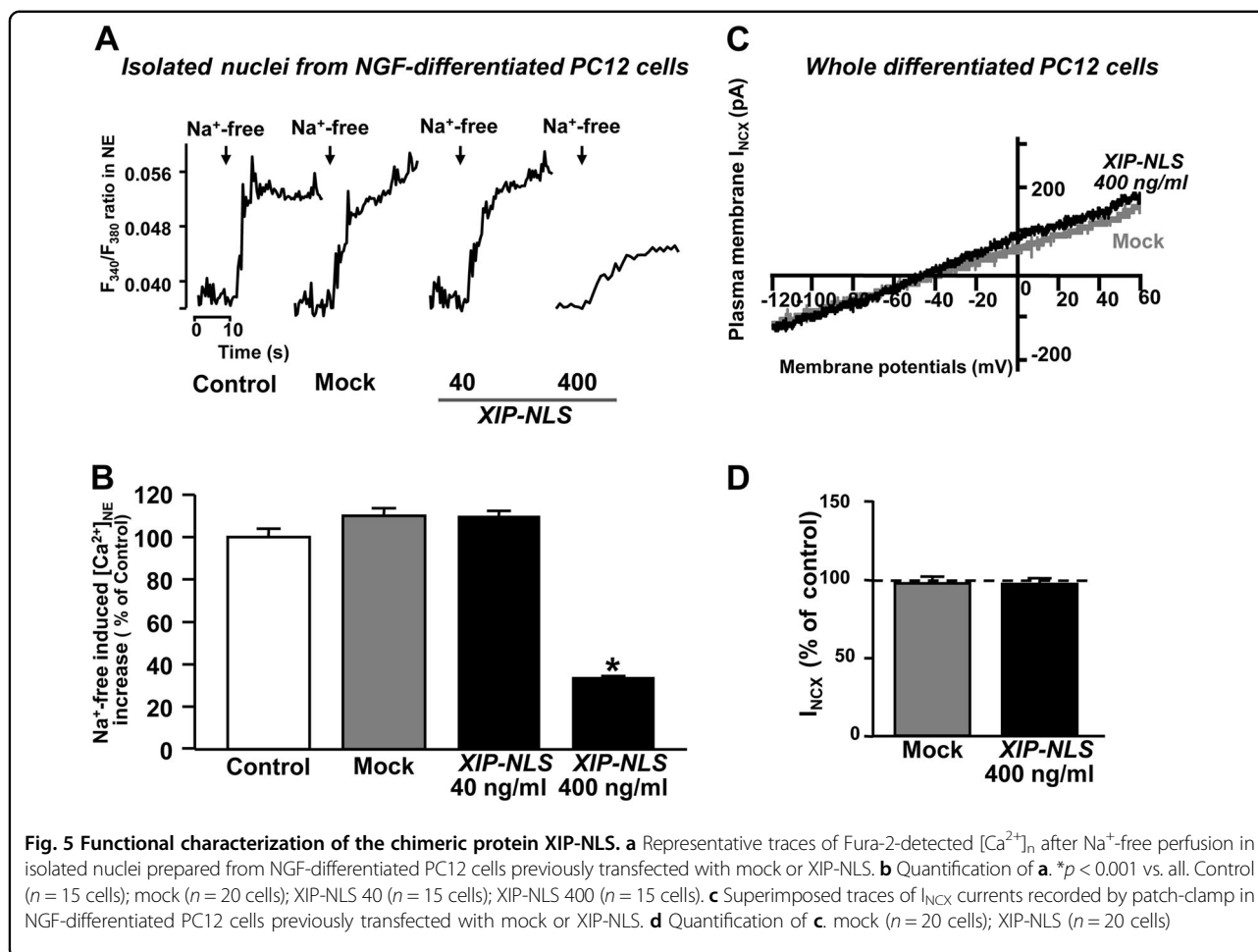


performed confocal double immunofluorescence experiments with the anti- β III-tubulin, a marker of immature neurons, and microtubule-associated protein-2 (MAP-2) that is expressed throughout all stages of neuronal differentiation. We found that the selective inhibition of nuclear NCX1 by transfecting XIP-NLS increased the percentage of β III-tubulin-positive immature neurons after 7 DIV compared with control cultures but did not change the percentage of MAP-2-positive neurons (Fig. 8b).

Discussion

The present study demonstrates that the nuclear $\text{Na}^+/\text{Ca}^{2+}$ exchanger isoform 1 (nuNCX1), located at the level of the inner membrane of NE (INM) in neurons, plays a relevant role in neuronal differentiation through the modulation of nuclear Ca^{2+} homeostasis. However, we found NCX1 immunosignal also outside the INM, possibly at the level of other intracellular organelles, whereas no detectable traces of the other two NCX isoforms, NCX2 and NCX3 were detected on INM. Compelling evidence for NCX1 specific localization to the INM is that, in nuclear preparations obtained from cortical neurons in which outer membrane was removed, nuNCX1 was co-expressed with specific markers of the INM, namely laminB1/B2 and CRM1. Furthermore, this specific

localization was paralleled by its specific activation. In particular, working in the forward mode of operation, nuNCX1 moved Ca^{2+} from the nucleoplasm to the NE lumen of neuronal cells. Indeed, NCX1 silencing, as well as the pharmacological inhibition of its activity by the amiloride derivative CB-DMB, abrogated Ca^{2+} rise in the lumen of NE due to the forward mode of the nuclear exchanger, thus demonstrating that nuNCX1 has the same pharmacological sensitivity of its plasmamembrane form. Therefore, nuNCX1 contributes to the Na^+ -dependent removal of $[\text{Ca}^{2+}]$ from nucleoplasm of neuronal cells. In this regard, we speculated that Ca^{2+} extrusion from the total nuclear compartment of a whole cell might entail two consecutive steps: the first step, operated by NCX1 located on the inner membrane of the NE, might mediate Ca^{2+} transport from the nucleoplasm to the lumen of the NE³⁰, and the second step, whose transporter mechanism is still unknown, might promote Ca^{2+} movement from the lumen of the nuclear envelope into the ER. Such new function might be supported by the presence of a Na^+ gradient existing between the lumen of the nuclear envelope and the nucleoplasm. Consistently, previous evidence indicates the presence of a Na^+ concentration gradient between the lumen (80 mM) and the nucleoplasm (5–20 mM), that is maintained by the nuclear form of the Na^+/K^+ ATPase³¹. Indeed, this pump is present in the



inner membrane of the nuclear envelope and is oriented with the ATP hydrolysis site in the nucleoplasm^{27,31}.

Indeed, the present finding is in line with our previous results demonstrating that NCX1 participates in NGF-induced neuronal differentiation via nuclear Akt²³. However, the present data seems to suggest that, among the different exchangers, nuNCX1 plays a major role in inducing neuronal differentiation working in the early phase of the process. Consistently, nuNCX1 expression and activity progressively increased during differentiation, thus peaking at 3 days of NGF exposure. At this time, nuNCX1 mainly controls nuclear-resident PTEN/Akt pathway via [Ca²⁺]_n modulation. Indeed, when we inhibited nuNCX1 with the chimeric fluorescent protein XIP-NLS, nuclear Ca²⁺ clearance decreased, whereas the [Ca²⁺]_n peak, elicited by ATP, increased. This effect on nucleoplasmic Ca²⁺ was due to the selective localization of XIP-NLS in the nucleus where it bound to the f-loop of nuNCX1, as also demonstrated by the coimmunoprecipitation between the peptide and nuNCX1 in isolated nuclei. Accordingly, the same interaction occurs at

plasma membrane NCX level²². Interestingly, XIP-NLS inhibited nuNCX1 Ca²⁺_n-extruding function without affecting the activity of plasma membrane NCX1, as demonstrated by patch-clamp experiments in whole neuronal cells. These data suggest that nuclear NCX1 plays a crucial role in regulating nuclear Ca²⁺ homeostasis upon [Ca²⁺]_i increase and works to remove nucleoplasmic Ca²⁺ accumulation in whole cell under physiological conditions.

Furthermore, the activity of nuNCX1 was involved in the regulation of PTEN/PI3K/Akt pathway, a transduction signal regulating neuronal differentiation. Moreover, during neuronal differentiation, the expression of PTEN, a phosphatase that converts phosphatidylinositol 3,4,5-trisphosphate to phosphatidylinositol 3,4-bisphosphate, was found to be inversely correlated to that of activated Akt. Specifically, the inhibition of nuNCX1 by XIP-NLS led to an increase in nuclear-resident PTEN expression and a decrease in Akt phosphorylation. Since nuNCX1, working in the forward mode, moves Ca²⁺ from nucleoplasm to NE lumen, it is conceivable that the blockade of

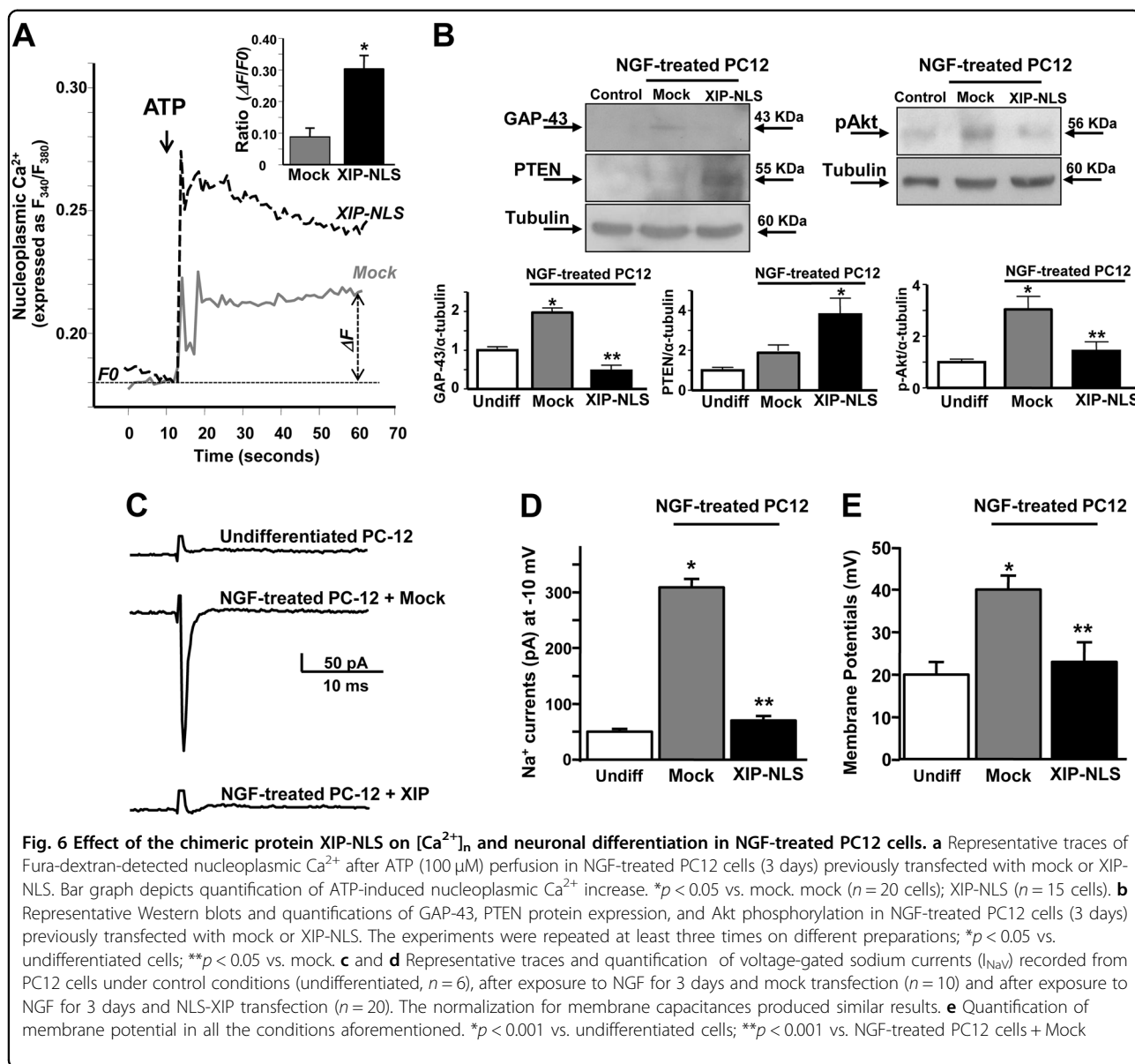
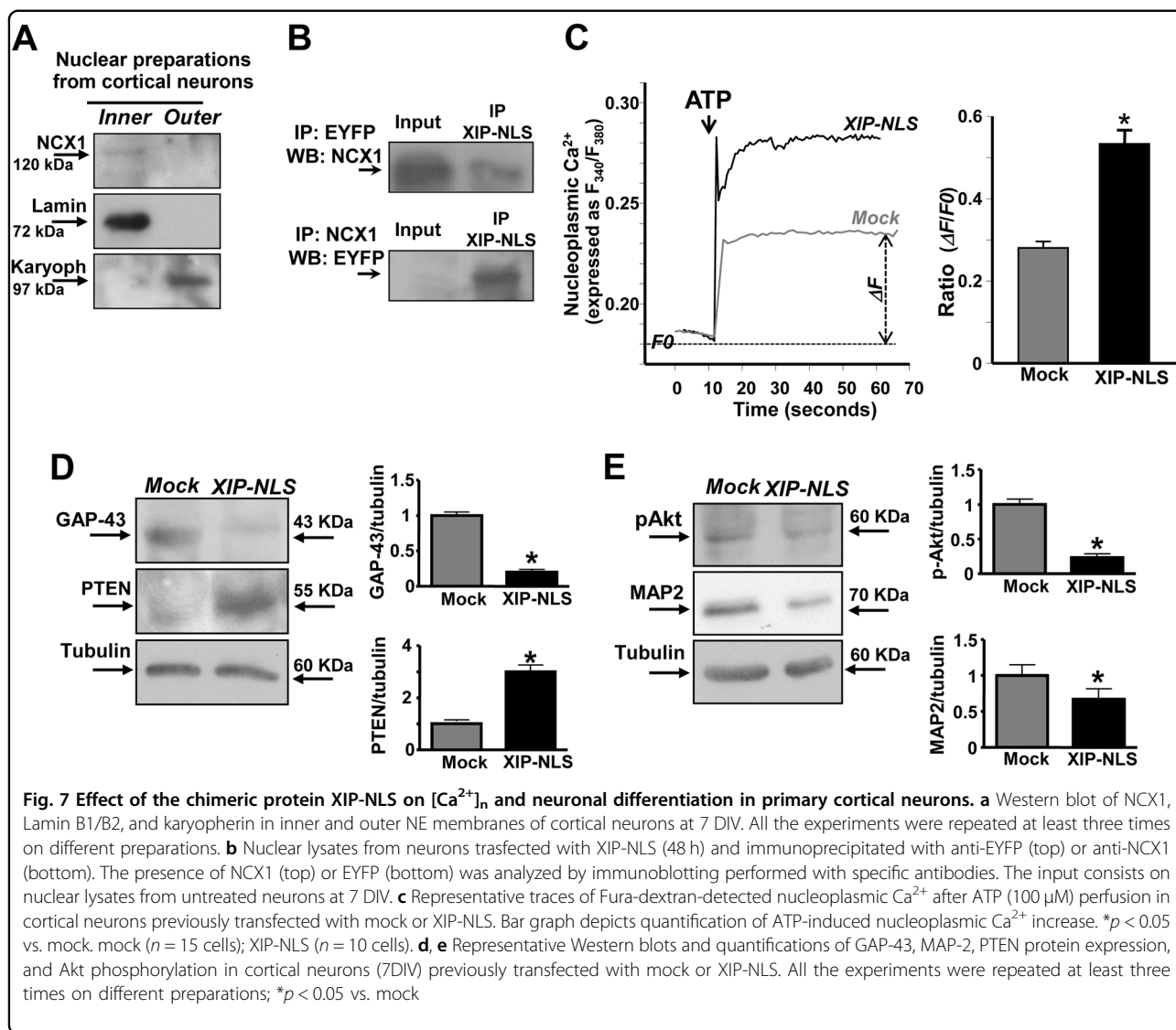


Fig. 6 Effect of the chimeric protein XIP-NLS on $[Ca^{2+}]_n$ and neuronal differentiation in NGF-treated PC12 cells. **a** Representative traces of Fura-dextran-detected nucleoplasmic Ca^{2+} after ATP (100 μ M) perfusion in NGF-treated PC12 cells (3 days) previously transfected with mock or XIP-NLS. Bar graph depicts quantification of ATP-induced nucleoplasmic Ca^{2+} increase. * $p < 0.05$ vs. mock. mock ($n = 20$ cells); XIP-NLS ($n = 15$ cells). **b** Representative Western blots and quantifications of GAP-43, PTEN protein expression, and Akt phosphorylation in NGF-treated PC12 cells (3 days) previously transfected with mock or XIP-NLS. The experiments were repeated at least three times on different preparations; * $p < 0.05$ vs. undifferentiated cells; ** $p < 0.05$ vs. mock. **c** and **d** Representative traces and quantification of voltage-gated sodium currents (I_{NaV}) recorded from PC12 cells under control conditions (undifferentiated, $n = 6$), after exposure to NGF for 3 days and mock transfection ($n = 10$) and after exposure to NGF for 3 days and NLS-XIP transfection ($n = 20$). The normalization for membrane capacitances produced similar results. **e** Quantification of membrane potential in all the conditions aforementioned. * $p < 0.001$ vs. undifferentiated cells; ** $p < 0.001$ vs. NGF-treated PC12 cells + Mock

this flux may promote, at nuclear level, a nucleoplasmic Ca^{2+} -dependent activation of nuclear-resident PTEN. Indeed, a part the well-established role in antagonizing PI3K signaling at the plasma membrane level, PTEN has been localized in the nucleus where it modulates transcriptional activity³². In addition, PTEN appears during elongation of growing neurites^{33,34}, and increases progressively at the early stage of differentiation, possibly to prevent aberrant neurite extension. In our study, once upregulated, PTEN was able to reduce Akt phosphorylation, MAP-2 and GAP-43 expression, thus avoiding neuronal differentiation in cortical neurons. Another interesting finding of this study is that XIP-NLS increased the percentage of β III-tubulin-positive immature neurons -after 7 DIV- in mature cultures of MAP-2-

positive cortical neurons, thus suggesting that the selective inhibition of nuNCX1 hampered neuronal differentiation of cortical neurons. This is in line with a very recent paper showing that the chronic treatment with NCX inhibitors produce marked reduction of the Purkinje cell dendritic arbor³⁵.

Collectively, this study unravels a new function for nuclear NCX1 within the complex regulatory machinery of nuclear calcium homeostasis, suggesting that this exchanger form may control neuronal differentiation through the fine regulation of Ca^{2+} -dependent transduction mechanisms.



Materials and methods

Cell cultures

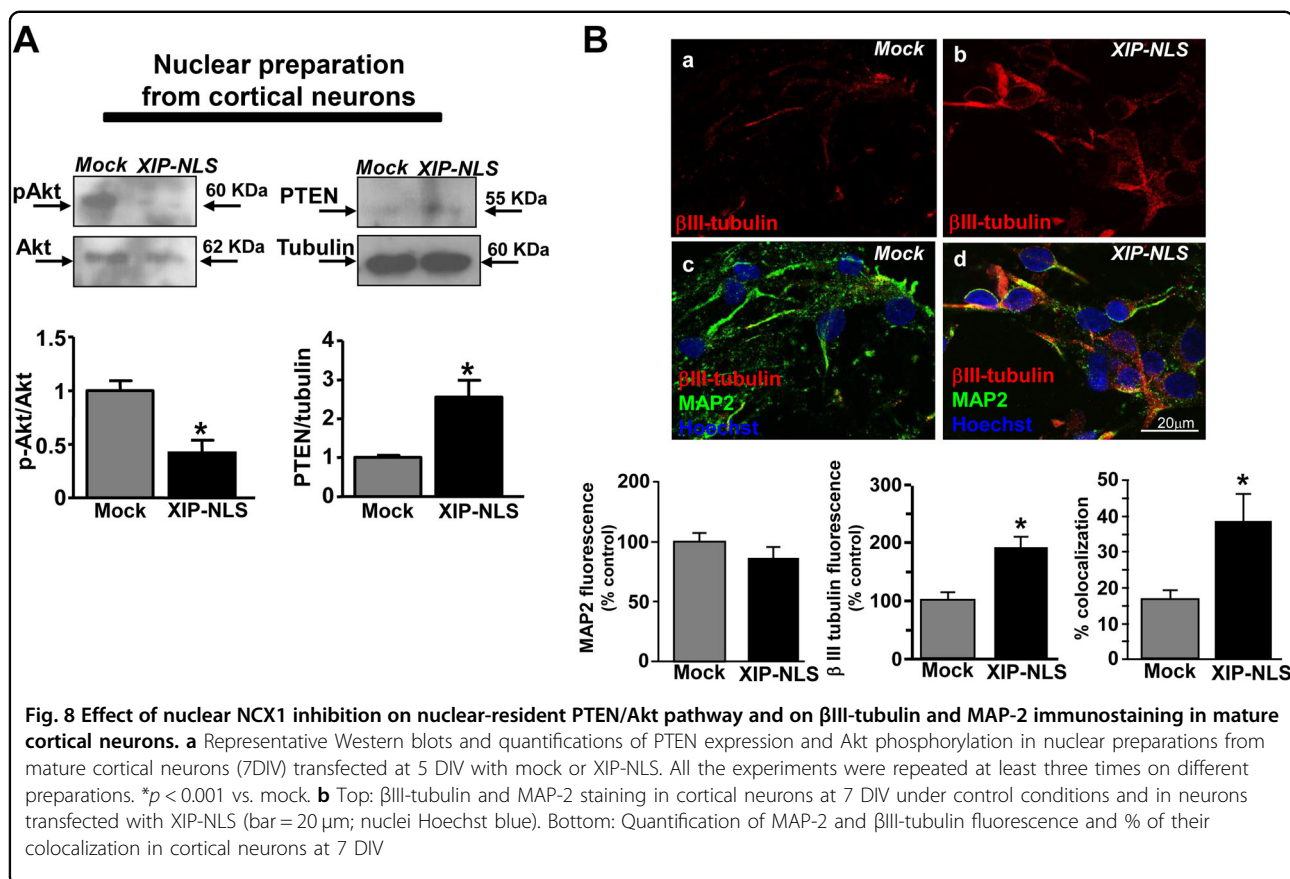
Clonal cells

PC12 cells were grown on plastic dishes in RPMI medium composed of 10% horse serum (HS), 5% fetal bovine serum (FBS), 100 UI/ml penicillin, and 100 μg/ml streptomycin. Neuronal differentiation was induced by exposing PC12 cells to NGF (50 ng/ml) were cultured in a humidified 5% CO₂ atmosphere. Culture medium was changed every 2 days. For functional studies, cells were seeded on glass coverslips (Fisher, Springfield, NJ, USA), coated with poly-L-lysine (5 μg/ml) (Sigma, St. Louis, Missouri, USA), and used at least 12 h after seeding.

Embryonic neurons

cortical pure neurons were prepared from brains of 16-day-old Wistar rat embryos. Briefly, the rats were first

anesthetized and then decapitated to minimize pain and distress. Dissection and dissociation were performed in Ca²⁺/Mg²⁺-free PBS containing glucose (30 mM). Tissues were incubated with papain for 10 min at 37 °C and dissociated by trituration in Earle's Balanced Salt Solution containing DNase, bovine serum albumin (BSA), and ovomucoid. Cells were plated at 15 × 10⁶ in 100-mm plastic Petri dishes pre-coated with poly-D-lysine (20 μg/ml) in minimum Eagle's medium/F12 (Life Technologies, Milan, Italy) containing glucose, 5% deactivated FBS, 5% deactivated HS (Life Technologies, Milan, Italy), glutamine, and antibiotics. Cytosine β-D-arabinofuranoside hydrochloride (Ara-C; 10 μM) was added within 48 h of plating to prevent non-neuronal cell growth. Neurons were cultured at 37 °C in a humidified 5% CO₂ atmosphere and used after 7 days of culture. All experiments on primary cortical neurons were performed according to



the procedures described in experimental protocols approved by the ethical committee of the “Federico II” University of Naples, Italy.

Isolation of intact nuclei

Highly purified nuclei were obtained from cell cultures by the combined use of hypotonic shock and mechanical disruption. Briefly, when they reached confluence, cells were washed twice in saline phosphate buffer and lysed in hypotonic buffer (10 mM Tris-HCl, pH 7.8, 10 mM β-mercaptoethanol, 0.5 mM phenylmethylsulfonyl fluoride (PMSF), 1 μg/ml aprotinin, leupeptin, and pepstatin). After 20 minutes on ice, the swollen samples were mechanically disrupted. The nuclear pellet was obtained by centrifugation at 500 g for 6 min at 4 °C and was then washed in a solution containing 10 mM Tris-HCl, 2 mM MgCl₂ plus protease inhibitors, pH 7.2. Finally, the nuclear pellet was resuspended in a standard solution (KCl 125 mM, HEPES 50 mM, K₂HPO₄ 2 mM, EGTA 0.1 mM, CaCl₂ 0.3 mM, NaCl 3 mM, containing 1 mM ATP, pH 7.4)^{11,34}. Nuclear preparations were used or stored at -80 °C until use. To check nuclear integrity, isolated nuclei were plated on glass coverslips (Fisher, Springfield, NJ, USA) previously coated with poly-L-lysine (30 μg/ml), and, then, fixed with 4% PAF (w/v) for 20 min at RT. After fixing, nuclear

preparations were stained with ethidium bromide and/or Nissl solution to study the purity, integrity, and possible ER contamination of nuclear preparations.

Inner and outer nuclear membranes separation

Freshly isolated nuclei of PC12 cells and cortical neurons were employed for isolation of NE as described previously¹⁸. Nuclear preparations were treated with 2% Na-citrate (trisodium, dihydrate) in a Nuclear Resuspension Buffer containing (in mM): 10 HEPES pH 7.9, 10 KCl, 1.5 MgCl₂, 0.1 EGTA, 0.5 DTT, 1 sodium orthovanadate (Na₃VO₄), 0.2 PMSF, 350 sucrose, protease inhibitors. Nuclei were pelleted by brief centrifugation at 5000×g: the pellet containing inner nuclear membranes was resuspended in nuclear resuspension buffer, while the supernatant containing outer nuclear membranes was precipitated with 10% trichloroacetic acid³⁶.

Nuclear/cytosolic fractionation and western blot analysis

Cytosolic and nuclear fractions were obtained from NGF-differentiated PC12 cells. In brief, cells were washed twice and collected in saline phosphate buffer by centrifugation at 1500 rpm for 3 min. Then, the pellet was dissolved in a buffer containing (in mM) 10 Hepes

pH 7.9, 10 KCl, 1.5 MgCl₂, 0.1 EGTA, 0.5 DTT, 1 sodium orthovanadate (Na₃VO₄), 0.2 PMSF, and protease inhibitors; the cytosolic fraction was then obtained by two consecutive centrifugations at 3000 rpm for 5 min at 4 °C. Nuclear fractions were obtained dissolving the pellet in a solution containing (in mM) 20 Hepes pH 7.9, 400 NaCl, 1.5 MgCl₂, 0.1 EGTA, 25% glycerol, 1 Na₃VO₄, 0.2 PMSF and protease inhibitors; throughout the procedure, the samples were kept on an agitation system for 30 min at 4 °C. Finally, samples were centrifuged at 13,000 rpm for 15 min.

For Western blot analysis, cell cultures, inner and outer nuclear membranes, and nuclear preparations were lysed with a buffer containing 20 mM Tris-HCl (pH 7.5), 10 mM NaF, 1 mM phenylmethylsulfonyl fluoride, 1% NONIDET P-40, 1 mM Na₃VO₄, 0.1% aprotinin, 0.7 mg/ml pepstatin, and 1 µg/ml leupeptin. Samples were cleared by centrifugation and supernatants were used for Western blot analysis. Protein concentration in supernatants was determined by the Bradford method³⁷. Protein samples (50 µg) were analyzed on 8% sodium dodecyl sulfate polyacrylamide gel with 5% sodium dodecyl sulfate stacking gel (SDS-PAGE) and electrotransferred onto Hybond ECL nitrocellulose papers (GE Healthcare, Little Chalfont, UK). Membranes were blocked with 5% non-fat dry milk in 0.1% Tween 20 (TBS-T; 2 mmol/l Tris-HCl, 50 mmol/l NaCl, pH 7.5) for 2 h at RT. Subsequently, they were incubated overnight at 4 °C in the blocked buffer containing the following antibodies: 1:1000 anti-NCX1 (rabbit polyclonal antibody, Swant, Bellinzona, Swiss), 1:1000 antibody for β-actin (mouse monoclonal antibody, Santacruz Biotechnology, Inc. CA), 1:500 anti-pAkt (mouse monoclonal antibody, Cell Signaling, Inc., MA, USA), 1:1000 anti-Akt (rabbit polyclonal antibody, Santa Cruz Biotechnology, Inc., CA, USA), 1:1000 anti-CRM1 (goat polyclonal antibody, Santa Cruz Biotechnology, Inc, CA, USA), 1:1000 anti-calretinin (rabbit polyclonal antibody; GeneTex, CA, USA), 1:500 anti-GAP-43 (mouse monoclonal antibody, Millipore Corporation, MA, USA), 1:1000 anti-MAP-2 (mouse monoclonal antibody, Sigma-Aldrich, Milan, Italy), 1:1000 anti-PTEN (mouse monoclonal antibody, Santa Cruz Biotechnology, Inc., CA, USA) and 1:2000 anti-α-tubulin (mouse monoclonal antibody, Sigma-Aldrich, Milan, Italy). Membranes were blocked with 5% non-fat dry milk in 0.1% Tween 20 (TBS-T; 2 mmol/l Tris-HCl, 50 mmol/l NaCl, pH 7.5) for 2 h at RT. Membranes containing nuclear fractions from neuronal cells treated with XIP-NLS were incubated overnight at 4 °C in the blocked buffer containing the following antibodies: 1:1000 anti-SOD1 (rabbit polyclonal anti-body, Santa Cruz Biotechnology, Inc., CA, USA), 1:1000 anti-GFP (mouse monoclonal anti-body, Abcam, Cambridge, UK), 1:1000 anti-CREB (mouse monoclonal anti-body, Cell Signaling Technology, Inc. MA, USA) and

pCREB (rabbit polyclonal anti-body, Millipore Corporation, MA, USA).

Membranes containing inner and outer nuclear fractions were incubated overnight at 4 °C in the blocked buffer containing the following antibodies: 1:1000 anti-NCX1 (rabbit polyclonal antibody, Swant, Bellinzona, Swiss); 1:200 anti-Lamin B1/B2 (mouse monoclonal antibody, Abcam, Cambridge, UK), 1:1000 calretinin (rabbit polyclonal antibody, GeneTex, Inc., GA, USA), and 1:1000 Karyopherin β2 (mouse monoclonal antibody, Santa Cruz Biotechnologies, Inc., CA, USA). Then, membranes were washed with 0.1% Tween 20 and incubated with the secondary antibodies (1:2000; GE Healthcare, Milan, Italy) for 1 h. Immunoreactive bands were detected using ECL reagent kits (GE Healthcare, Milan, Italy). The optical density of the bands was determined by Chemi-Doc Imaging System (Bio-Rad Laboratories, Milan, Italy).

qRT-PCR analysis

qRT-PCR was performed in a 7500-fast real-time PCR system (Applied Biosystems) by Fast SYBR Green Master Mix (Applied Biosystems). Samples were amplified simultaneously in triplicate as follows: heating 2 min at 50 °C, denaturation 10 min at 95 °C, amplification and quantification 35 cycles of 15 s at 95 °C; 1 min at 60 °C with a single fluorescence measurement. The data were normalized by using hypoxanthine phosphor-ribosyl-transferase (HPRT) as an internal control. Differences in mRNA content between groups were expressed by using 2^{-ΔΔCt} formula. The oligonucleotide sequences were for NCX1, forward: AGATTC CGTGACTGCAGTTGTG and reverse: ATACTGGTCCT GGGTAGCTGCTA; for NCX3, forward: CGGTACACAG CTGTTGTTTTTGT and reverse: CAGGGCAGCAGCTT TGCT; for HPRT, forward: TGGAAAGAACGTCTTG ATTGTTGA and reverse: GCTGTACTGCTTGACC AAGGAA.

Small interfering RNA

NCX1 knock down was achieved with siRNA duplexes against NCX1 and its non-targeting control (Invitrogen, San Giuliano Milanese, Milan, IT). The following gene-specific sequences were used successfully:

(RNA)-CCAAAUGGAGAGACCACCAAGACU and (RNA)-UAGUCUUGGUGGUCUCUCCAUUUGG or (RNA)-AC AUGUCCUCGGAGUUUCUAUUUAU and (RNA)-AUA AUAGAAACUCCGAGGAACAUGU. After 5 days in culture with NGF, PC12 cells were transfected for 5 h with each duplex at a final concentration of 10 nM using HyPerFect transfection reagent (Qiagen, Milan, IT).

Generation and expression of XIP-NLS

The expressing vector encoding for XIP-NLS protein was obtained by sub-cloning in frame 2 copies of each XIP

and NLS cDNAs in EYFP-C3 plasmid (Clontech Laboratories, Mountain View, CA), as shown in Fig. 4 panel A. In particular, 2 copies of the cDNA (from rat NCX1.1 NM_019268.3) encoding for XIP domain (DRRLFYKY-VYKRYRAGKQR) were obtained by PCR on a single plasmid and digested by specific restriction enzymes, whereas the two cDNAs encoding for NLS (from SV40 Large T-anti-gen) and a translational stop codon (PKKKRKV*) were obtained by in vitro annealing of two synthetic oligodeoxy nucleotide strains (Eurofinsgenomics, Ebersberg, Germany). Both XIP and NLS cDNAs were sequentially ligated in frame in the multicloning site of the EYFP-C3 plasmid. Two or more neutral aminoacids separated EYFP, XIP, and NLS domains. Successful construction of the plasmid encoding for YFP-XIP-NLS was verified by sequencing both strands (Microgem, Naples, Italy). This plasmid named XIP-NLS was transiently transfected in PC12 cells with Lipofectamine 2000 (Invitrogen, Carlsbad, CA), according to the manufacturer's protocol. The efficiency of transfection was calculated by counting the number of EYFP-positive nuclei compared to total Hoechst-positive nuclei.

Immunoprecipitation analyses

Cortical neurons were transfected with an excess of XIP-NLS (400 ng/ml). After transfection, nuclei from each population were isolated as previously described and homogenized in lysis buffer containing: 50 mM HEPES, 100 mM NaCl, 1.5 mM MgCl₂, 1 mM PMSF, 0.2% Nonidet P-40, 5 µg/ml aprotinin, 10 µg/ml leupeptin and 2 µg/ml pepstatin. The nuclear lysates were cleared by centrifugation at 12,000 rpm for 10 min. At the end, 1 mg of nuclear lysate was immunoprecipitated with the mouse monoclonal anti-EGFP antibody (1:200) or the rabbit polyclonal anti-NCX1 antibody (1:200). Then, the immunoprecipitates were resolved by Western Blotting and immunoblot analysis was performed using anti-NCX1 or anti-GFP antibodies, respectively.

Immunocytochemistry

Isoform-specific antibodies for NCX1 and Lamin B1/B2, alone or in combination, were used for immunocytochemistry. The rabbit polyclonal anti-NCX1 antibody was purchased from Swant (Bellinzona, Switzerland). Cells or isolated nuclei were rinsed twice in cold 0.01 M saline phosphate buffer (PBS) at pH 7.4 and fixed in 4% (w/v) paraformaldehyde (Sigma, Milan, Italy) for 20 min at RT. Following three washes in PBS, cells were blocked with 3% (w/v) BSA and 0.05% Triton-X (Biorad, Milan, Italy) for 1 h at RT. The coverslips were then incubated overnight with the primary antibody anti-NCX1 (1:1000 dilution), or anti-Lamin B1/B2 (1:50, Abcam, UK). After three washes in PBS, the coverslips were incubated in the dark for 1 h at RT with two secondary antibodies: Cy2 anti-mouse IgG

and Cy3 anti-rabbit IgG (1:200, Jackson Immuno Research Laboratories, Inc. PA, USA). The immunosignal of NCX1 shown in Fig. 1 panel A and Fig. 2 panel A was detected by using a biotinylated secondary antibody. After this latter incubation, the peroxidase reaction was developed using 3,3'-diaminobenzidine/4-HCl as a chromogen. Then, after the final wash, coverslips were mounted with Vectashield (Vector Labs, Burlingame, CA). Fluorescence intensity of MAP2 and βIII-tubulin in cortical neurons was quantified in terms of pixel intensity value by using the NIH image software. Briefly, digital images were taken with 63x objective and identical laser power settings and exposure times were applied to all the photographs from each experimental set. The quantification of colocalization between MAP2 and βIII-tubulin was assessed by using the 'co-localization highlighter' plug-in for ImageJ Software (NIH, Bethesda, MA, USA). Before colocalization analysis, threshold settings for each image were determined, and quantification was achieved by counting the number colocalized points per microscope field. Results were expressed as a percentage of colocalization. All images were observed using a Zeiss LSM510 META/laser-scanning confocal microscope.

[Ca²⁺]_i and nuclear Ca²⁺ measurements

[Ca²⁺]_i was measured by single-cell computer-assisted video-imaging in isolated nuclei from NGF-differentiated PC12 loaded with Fura-2/AM (Calbiochem)^{38,39}. Under these conditions, Fura-2 is trapped within the NE lumen. However, nucleoplasmic Ca²⁺ was measured in whole cells by loading NGF-differentiated PC12 with Fura-1dextran (10 µM/1 h at 37 °C in the presence of 0.05% Pluronic), a conjugated form of the fluorescent probe that is trapped in the nucleoplasmic space.

To perform functional analysis of Ca²⁺ level in the lumen of NE on isolated nuclei, we modified the methods used by Gerasimenko et al.¹¹ and Xie et al.¹⁸. Fresh nuclear preparations from NGF-differentiated PC12 cells were placed on glass coverslips previously treated with 30 µg/ml poly-L-lysine. After 1 h, the preparation was loaded with 10 µM Fura-2/AM at 4 °C in a standard solution containing 0.04% Pluronic. At the end of the Fura-2/AM loading period, isolated nuclei were allowed to settle for 15 min in a TM solution composed of: 20 mM Tris-HCl, 1 mM MgCl₂, 150 mM NaCl with a pH of 7.4 and then subjected to an uptake buffer named Na⁺-free consisting of: 250 mM sucrose, 50 mM Tris-HCl, 4 mM K₂HPO₄, 4 mM MgCl₂, 2 mM EGTA, 2 mM EDTA, and 147 mM NMDG⁺ together with 2.5 mM CaCl₂, pH 7.4¹⁸. To measure Ca²⁺ levels, both in whole cells and isolated nuclei, coverslips were placed into a perfusion chamber (Medical System, Co. Greenvale, NY, USA) mounted onto a Zeiss Axiovert 200 microscope (Carl Zeiss, Germany) equipped with a FLUAR 40X oil objective lens. The

experiments were carried out with a digital imaging system composed of MicroMax 512BFT cooled CCD camera (Princeton Instruments, Trenton, NJ, USA), LAMBDA 10-2 filter wheel (Sutter Instruments, Novato, CA, USA), and Meta-Morph/MetaFluor Imaging System software (Universal Imaging, West Chester, PA, USA). After loading, nuclei were alternatively illuminated at wavelengths of 340 and 380 nm by a Xenon lamp. The emitted light was passed through a 512 nm barrier filter. Fura-2 fluorescence intensity was measured every 3 s and reported as F340/F380 ratios.

For the experiments of Figs. 6 and 7, NGF-differentiated PC12 cells and cortical neurons at 7 DIV were illuminated at wavelengths of 480 nm to identify EYFP-positive cells and then at 340 and 380 nm to measure, in the EYFP-positive cells, Fura-dextran-detected nucleoplasmic Ca^{2+} levels. Ca^{2+} levels have been reported as 340/380 ratio.

Electrophysiological recording of NCX and voltage-gated sodium channel activity by patch clamp

The membrane voltage and current were acquired using pClamp10 software.

Plasma membrane NCX currents (I_{NCX}) in NGF-differentiated PC12 cells were recorded by the patch-clamp technique in whole-cell configuration using the commercially available amplifier Axopatch200B and Digidata1322A interface (Molecular Devices), as previously described^{28,40}. I_{NCX} were recorded starting from a holding potential of -60 mV up to a short-step depolarization at $+60$ mV (60 ms). A descending voltage ramp from $+60$ mV to -120 mV was applied. I_{NCX} recorded in the descending portion of the ramp (from $+60$ mV to -120 mV) were used to plot the current-voltage (I - V) relation curve. The I_{NCX} magnitude was measured at the end of $+60$ mV (reverse mode) and at the end of -120 mV (forward mode), respectively. The Ni^{2+} -insensitive component was subtracted from total currents to isolate I_{NCX} ^{21,41}. Neuronal cells were perfused with external Ringer's solution containing the following (in mM): 126 NaCl, 1.2 NaHPO₄, 2.4 KCl, 2.4 CaCl₂, 1.2 MgCl₂, 10 glucose, and 18 NaHCO₃, pH 7.4. Twenty millimolar tetraethylammonium (TEA), 50 nM TTX, and 10 μM nimodipine were added to Ringer's solution to abolish potassium, sodium, and calcium currents. The dialyzing pipette solution contained the following (in mM): 100 K-gluconate, 10 TEA, 20 NaCl, 1 Mg-ATP, 0.1 CaCl₂, 2 MgCl₂, 0.75 EGTA, and 10 HEPES, adjusted to pH 7.2 with CsOH.

For tetrodotoxin (TTX)-sensitive Na^{+} channel recordings, NGF-differentiated PC12 cells and untreated PC12 cells were perfused with an extracellular Ringer's solution containing 20 mM tetraethylammonium (TEA) and 5 μM nimodipine. The pipettes were filled with 110 mM CsCl, 10 mM TEA, 2 mM MgCl₂, 10 mM EGTA, 8 mM glucose, 2 mM Mg-ATP, 0.25 mM cAMP, and 10 mM HEPES (pH

7.3). TTX-sensitive Na^{+} currents were recorded as previously described by Secondo et al.²³. The mean resting membrane potential (holding potential at 0 current) was measured using the above-mentioned bath solution in absence of TTX and TEA. Capacitive currents were estimated from the decay of the capacitive transient induced by 5 mV depolarizing pulses from a holding potential of -80 mV and acquired at a sampling rate of 50 kHz. The capacitance of the membrane was calculated according to the following equation: $C_m = \tau_c \cdot I_0 / \Delta E_m (1 - I_\infty / I_0)$, where C_m is membrane capacitance, τ_c is the time constant of the membrane capacitance, I_0 is the maximum capacitance current value, ΔE_m is the amplitude of the voltage step, and I_∞ is the amplitude of the steady state current.

Statistical analysis

Data are expressed as mean \pm S.E.M. Statistical comparisons between controls and treated experimental groups were performed using the one-way ANOVA, followed by Newman Keul's test. $p < 0.05$ was considered statistically significant.

Acknowledgements

This work was supported by PON01_01602 and PON03PE_00146_1 by MIUR to L.A., Progetto Giovani Ricercatori GR-2010-2318138 from Ministero della Salute and PRIN 2015 from MIUR to A.S., Futuro in Ricerca 2013 (RBFR13M6FN) from MIUR to P.M., and Fondazione Italiana Sclerosi Multipla FISM 2015/R/6 to F.B. We thank Dr. Paola Merolla for the editorial revision.

Author contributions

AS designed the study, performed video-imaging, interpreted results and wrote the first draft of the manuscript. TP performed Western blot experiments, NE isolation and NE membranes separation. FB assisted with immunohistochemistry and interpreted the results. AE and VT performed biochemical experiments while NG performed qRT-PCR. PM designed and generated XIP-NLS expressing vector; RC and AP performed electrophysiological measurements. LA and GF assisted with designing experiments and, interpreting results, edited the manuscript. All authors read and approved the final manuscript. All experiments were performed at "Federico II" University of Naples, Italy.

Competing interests

The authors declare that they have no competing interests.

Publisher's note

Springer Nature remains neutral with regard to jurisdictional claims in published maps and institutional affiliations.

Received: 23 October 2017 Accepted: 25 November 2017

Published online: 30 April 2018

References

1. Bootman, M. D., Fearnley, C., Smyrniak, I., MacDonald, F. & Roderick, H. L. An update on nuclear calcium signalling. *J. Cell. Sci.* **122**, 2337–2350 (2009).
2. Rodrigues, M. A. et al. Nucleoplasmic calcium is required for cell proliferation. *J. Biol. Chem.* **282**, 17061–17068 (2007).

3. Pusch, T. et al. Epidermal growth factor-mediated activation of the ETS domain transcription factor Elk-1 requires nuclear calcium. *J. Biol. Chem.* **277**, 27517–27527 (2002).
4. Ledo, F., Kremer, L., Mellstrom, B. & Naranjo, J. R. Ca²⁺-dependent block of CREB-CBP transcription by repressor DREAM. *Embo. J.* **21**, 4583–4592 (2002).
5. Delivoria-Papadopoulos, M., Akhter, W. & Mishra, O. P. Hypoxia-induced Ca²⁺-influx in cerebral cortical neuronal nuclei of newborn piglets. *Neurosci. Lett.* **342**, 119–123 (2003).
6. Delivoria-Papadopoulos, M., Ashraf, Q. M. & Mishra, O. P. Effect of hypoxia on expression of apoptotic proteins in nuclear, mitochondrial and cytosolic fractions of the cerebral cortex of newborn piglets: the role of nuclear Ca²⁺-influx. *Neurochem. Res.* **33**, 1196–1204 (2008).
7. Leite, M. F. et al. Nuclear and cytosolic calcium are regulated independently. *Proc. Natl. Acad. Sci.* **100**, 2975–2980 (2003).
8. Nicotera, P., Orrenius, S., Nilsson, T. & Berggren, P. O. An inositol 1,4,5-trisphosphate-sensitive Ca²⁺ pool in liver nuclei. *Proc. Natl. Acad. Sci.* **87**, 6858–6862 (1990).
9. Stehno-Bittel, L., Luckhoff, A. & Clapham, D. E. Calcium release from the nucleus by InsP3 receptor channels. *Neuron* **14**, 163–167 (1995).
10. Bezin, S., Fossie, P. & Cancela, J. M. Nucleoplasmic reticulum is not essential in nuclear calcium signalling mediated by cyclic ADPrbose in primary neurons. *Pflug. Arch.* **456**, 581–586 (2008).
11. Gerasimenko, O. V., Gerasimenko, J. V., Tepikin, A. V. & Petersen, O. H. ATP-dependent accumulation and inositol trisphosphate- or cyclic ADPrbose-mediated release of Ca²⁺ from the nuclear envelope. *Cell* **80**, 439–444 (1995).
12. Campden, R., Audet, N. & Hébert, T. E. Nuclear G protein signaling: new tricks for old dogs. *J. Cardiovasc. Pharm.* **65**, 110–122 (2015).
13. Mazzanti, M., Bustamante, J. O. & Oberleithner, H. Electrical dimension of the nuclear envelope. *Physiol. Rev.* **81**, 1–19 (2001).
14. Tabares, L., Mazzanti, M. & Clapham, D. E. Chloride channels in the nuclear membrane. *J. Membr. Biol.* **123**, 49–54 (1991).
15. Bkaily, G. et al. The use of confocal microscopy in the investigation of cell structure and function in the heart, vascular endothelium and smooth muscle cells. *Mol. Cell. Biochem.* **172**, 171–194 (1997).
16. Bkaily, G. et al. G-protein-coupled receptors, channels, and Na⁺-H⁺ exchanger in nuclear membranes of heart, hepatic, vascular endothelial, and smooth muscle cells. *Can. J. Physiol. Pharm.* **84**, 431–441 (2006).
17. Abrenica, B. & Gilchrist, J. S. Nucleoplasmic Ca²⁺ loading is regulated by mobilization of perinuclear Ca²⁺. *Cell. Calcium* **28**, 127–136 (2000).
18. Xie, X., Wu, G., Lu, Z. H. & Ledeen, R. W. Potentiation of a sodium-calcium exchanger in the nuclear envelope by nuclear GM1 ganglioside. *J. Neurochem.* **81**, 1185–1195 (2002).
19. Ledeen, R. & Wu, G. GM1 in the nuclear envelope regulates nuclear calcium through association with a nuclear sodium-calcium exchanger. *J. Neurochem.* **103**, 126–134 (2007).
20. Annunziato, L., Pignataro, G. & Di Renzo, G. F. Pharmacology of brain Na⁺-Ca²⁺ exchanger: from molecular biology to therapeutic perspectives. *Pharm. Rev.* **56**, 633–654 (2004).
21. Molinaro, P. et al. Na⁺-Ca²⁺ exchanger (NCX3) knock-out mice display an impairment in hippocampal long-term potentiation and spatial learning and memory. *J. Neurosci.* **31**, 7312–7321 (2011).
22. Molinaro, P. et al. Neuronal NCX1 overexpression induces stroke resistance while knockout induces vulnerability via Akt. *J. Cereb. Blood. Flow. Metab.* **36**, 1790–1803 (2016).
23. Secondo, A. et al. Involvement of the Na⁺/Ca²⁺ exchanger isoform 1 (NCX1) in neuronal growth factor (NGF)-induced neuronal differentiation through Ca²⁺-dependent Akt phosphorylation. *J. Biol. Chem.* **290**, 1319–1331 (2015).
24. Zou, H. et al. MicroRNA-29A/PTEN pathway modulates neurite outgrowth in PC12 cells. *Neurosci.* **29**, 289–300 (2015).
25. van Diepen, M. T. & Eickholt, B. J. Function of PTEN during the formation and maintenance of neuronal circuits in the brain. *Dev. Neurosci.* **30**, 59–64 (2008).
26. Zhou, J. & Parada, L. F. PTEN signaling in autism spectrum disorders. *Curr. Opin. Neurobiol.* **22**, 873–879 (2012).
27. Galva, C., Artigas, P. & Gatto, C. Nuclear Na⁺/K⁺-ATPase plays an active role in nucleoplasmic Ca²⁺ homeostasis. *J. Cell. Sci.* **125**, 6137–6147 (2012).
28. Secondo, A. et al. Molecular pharmacology of the amiloride analog 3-amino-6-chloro-5-[[4-chloro-benzyl]amino]-n-[[[2,4-dimethylbenzyl]-amino]imino-methyl]-pyrazinocarboxamide (CB-DMB) as a pan inhibitor of the Na⁺-Ca²⁺ exchanger isoforms NCX1, NCX2, and NCX3 in stably transfected cells. *J. Pharm. Exp. Ther.* **331**, 212–221 (2009).
29. Savard, M. et al. Expression of endogenous nuclear bradykinin B2 receptors mediating signaling in immediate early gene activation. *J. Cell. Physiol.* **216**, 234–244 (2008).
30. Wu, G., Xie, X., Lu, Z. H. & Ledeen, R. W. Sodium-calcium exchanger complexed with GM1 ganglioside in nuclear membrane transfers calcium from nucleoplasm to endoplasmic reticulum. *Proc. Natl. Acad. Sci.* **106**, 10829–10834 (2009).
31. Garner, M. H. Na,K-ATPase in the nuclear envelope regulates Na⁺ K⁺ gradients in hepatocyte nuclei. *J. Membr. Biol.* **187**, 97–115 (2002).
32. Freeman, D. J. et al. PTEN tumor suppressor regulates p53 protein levels and activity through phosphatase-dependent and -independent mechanisms. *Cancer Cell.* **3**, 117–130 (2003).
33. Musatov, S. et al. Inhibition of neuronal phenotype by PTEN in PC12 cells. *Proc. Natl. Acad. Sci.* **101**, 3627–3631 (2004).
34. Gerasimenko, J., Maruyama, Y., Tepikin, A., Petersen, O. H. & Gerasimenko, O. Calcium signalling in and around the nuclear envelope. *Biochem. Soc. Trans.* **31**, 76–78 (2003).
35. Sherkhane, P. & Kapfhammer, J. P. Chronic pharmacological blockade of the Na⁺/Ca²⁺ exchanger modulates the growth and development of the Purkinje cell dendritic arbor in mouse cerebellar slice cultures. *Eur. J. Neurosci.* **46**, 2108–2120 (2017).
36. Gilchrist, J. S. & Pierce, G. N. Identification and purification of a calcium-binding protein in hepatic nuclear membranes. *J. Biol. Chem.* **268**, 4291–4429 (1993).
37. Bradford, M. M. A rapid and sensitive method for the quantification of microgram quantities of protein utilizing the principle of protein-dye binding. *Ann. Biochem.* **72**, 248–254 (1976).
38. Gryniewicz, G., Poenie, M. & Tsien, R. Y. A new generation of Ca²⁺ indicators with greatly improved fluorescence properties. *J. Biol. Chem.* **260**, 3440–3450 (1985).
39. Secondo, A. et al. BHK cells transfected with NCX3 are more resistant to hypoxia followed by reoxygenation than those transfected with NCX1 and NCX2: Possible relationship with mitochondrial membrane potential. *Cell. Calcium* **42**, 521–535 (2007).
40. Pannaccione, A. et al. A new concept: Aβ1-42 generates a hyperfunctional proteolytic NCX3 fragment that delays caspase-12 activation and neuronal death. *J. Neurosci.* **32**, 10609–10617 (2012).
41. Molinaro, P. et al. Neurounina-1, a novel compound that increases Na⁺/Ca²⁺ exchanger activity, effectively protects against stroke damage. *Mol. Pharm.* **83**, 142–156 (2013).